Applied Mathematics and Computation 291 (2016) 98–114

Contents lists available at ScienceDirect

Applied Mathematics and Computation

journal homepage: www.elsevier.com/locate/amc

Development lengths in Newtonian Poiseuille flows with wall slip

Zacharias Kountouriotis, Maria Philippou, Georgios C. Georgiou*

Department of Mathematics and Statistics, University of Cyprus, P.O. Box 20537, 1678 Nicosia, Cyprus

ARTICLE INFO

Keywords:
Newtonian fluid
Slip
Poiseuille flow
Development length
Wall development length
Finite elements

ABSTRACT

The effect of wall slip on the development of planar and axisymmetric Newtonian Poiseuille flows is studied by means of finite element simulations. The Navier slip law is employed. i.e., it is assumed that the slip velocity varies linearly with the wall shear stress. In addition to the standard definition of the development length, L, as the length required for the maximum velocity to attain 99% of its fully-developed value, the wall development length L_w is also relevant in the presence of slip. This is defined as the length required for the slip velocity to decrease to 1.01% of its fully-developed value. The numerical simulations for the planar and the axisymmetric geometries showed that both L and L_w increase with slip passing through a maximum and vanish at a critical value of the slip parameter corresponding to the full slip case. Moreover, the velocity overshoots and the axial pressure minimum near the entrance become less pronounced as slip becomes stronger. The calculations of L for the planar flow are in good agreement with available results in the literature. An interesting result is that in contrast to the axisymmetric flow in which $L_w < L$, the planar flow develops more slowly at the wall than at the midplane, i.e. $L_w > L$ in the planar case.

1. Introduction

The classical Newtonian Poiseuille flow development or entry flow problem in tubes of various cross sections is still the subject of research not only because it finds applications in viscometry, in micro-/nano-fluidics and in biomechanics [1,2], but also due to its relevance concerning transition to turbulence [3]. The flow development region is very important particularly in microchannels, since these are usually very short and thus pressure drop and heat transfer are very different from their fully-developed counterparts [4,5]. The analysis of pressure loss in the flow development region is also required in the design of flow-intake devices. The main parameter of interest is the development or entrance length, L^*, defined as the length required for laminar pipe flow to fully develop from a uniform to the standard parabolic distribution. In practice, the development length is most commonly defined as the length required for the cross-sectional maximum velocity to attain 99% of its fully developed value [6].

The main factor affecting the development length of laminar, incompressible Newtonian flow is inertia. The dimensionless development length is defined by

$$L \equiv \frac{L^*}{L_s^*} \tag{1}$$

* Corresponding author. Tel.: +357 22892612; fax: +357 22895352.
E-mail address: georgios@ucy.ac.cy (G.C. Georgiou).

http://dx.doi.org/10.1016/j.amc.2016.06.041
0096-3003/

where L_s^* is a characteristic length, i.e. the diameter D^* for a pipe or the slit gap $2H^*$ for a channel. The development length is a function of the Reynolds number, *Re*, which is defined using the same characteristic length:

$$Re \equiv \frac{\rho^* U^* L_s^*}{\mu^*} \tag{2}$$

where ρ^* is the density, U^* is the mean velocity, and μ^* is the viscosity. It should be indicated that throughout this paper dimensional quantities are denoted by starred symbols and thus symbols without stars correspond to dimensionless quantities and numbers.

Both experiments [7] and numerical calculations [8] have shown that in circular pipes the ratio L/Re is a decreasing function of *Re* for $Re < 200$ and practically constant otherwise. Atkinson et al. [9] proposed correlations of the form

$$L = C_0 + C_1 Re \tag{3}$$

for pipes and channels, where C_0 and C_1 are positive constants, in order to combine the high Reynolds number asymptotes and the creeping flow limits. The constant C_0 corresponds to the creeping flow development length and is about 0.6 for either geometry [2]. A number of other correlations have also been proposed, such as those of Shah and London [6] or those of Dombrowski et al. [10] and Durst et al. [11], which give a better fit to the data of Friedman et al. [8] in the range $0 < Re < 100$. Similar correlations have also been proposed for channels with rectangular cross-sections [2], which indicate that the high Reynolds number asymptote (i.e., C_1) decreases with increasing aspect ratio. Nevertheless, as pointed out by Boger [12] and Sinclair [2], the use of these correlations is questionable for low *Re*.

Studies concerning the flow development of non-Newtonian flows have also been reported [13]. The development of laminar flow of power-law fluids and Bingham plastics in a pipe has been studied numerically by Poole and Ridley [14] and Poole and Chhabra [15], respectively. More recently, Ferrás et al. [16] reported numerical results for the flow development of a Sisco fluid in a channel. Yapici et al. [17] also analyzed numerically the developing flow of Oldroyd-B and Phan-Thien–Tanner (PTT) fluids through a two-dimensional rectangular channel.

The no-slip condition is one of the main assumptions made in the classical entry flow problem. It is this condition that causes the fluid layers close to the wall to be retarded by viscous action and form a thin boundary layer the thickness of which grows downstream till the flow becomes fully developed. However, as pointed out by Neto et al. [4], slip is important in entry flows in microfluidic and nanofluidic devices even for Newtonian flows. Recently, Ferrás et al. [1] studied the effect of wall slip on the development length in the case of channel flow. In their study, they employed the Navier slip law [18], which relates linearly the wall shear stress, τ_w^*, to the slip velocity, u_w^*, defined as the relative velocity of the fluid with respect to that of the wall:

$$\tau_w^* = \beta^* u_w^* \tag{4}$$

where β^* is the slip coefficient, which depends in general on temperature, normal stress and pressure, and the characteristics of the fluid/wall interface [19]. The no-slip and perfect-slip cases are recovered when $\beta^* \to \infty$ and $\beta^* = 0$, respectively. Ferrás et al. [1] showed the decisive influence of slip on the development length which increases with wall slip only initially exhibiting a maximum.

The main objective of the present work is to investigate the effect of wall slip in the case of a circular tube which is more important in applications. Since the velocity at the wall is not zero, it is also interesting to check if there are cases where the flow at the wall develops more slowly than at the symmetry axis. In such a case, the use of an alternative definition of the development length is obviously more appropriate. Hence, the dimensionless wall development length, L_w, is hereby defined as the length required for the slip velocity to decrease down to 1.01% of its fully developed value, and make comparisons between L and L_w for both the axisymmetric and planar configurations. Note that only low and moderate Reynolds numbers are considered, in the range 0-400, which is relevant to microfluidic devices.

The effect of slip in gas flow development in the entrance of circular and non-circular microchannels has been studied by Duan and Muzychka [20], who solved a linearized momentum equation and developed an asymptotic model for predicting the friction factor and Reynolds product with an approximate accuracy of 10% for most common duct shapes. It should be pointed out that the present work concerns liquid and non gas-flow development. Moreover, the full non-linear momentum equation is considered and solved numerically.

The rest of the paper is organized as follows. In Section 2, the dimensionless governing equations are presented. In Section 3, the numerical method is briefly described and the numerical results are discussed. Finally, the main conclusions of this work are summarized in Section 4.

2. Governing equations

We consider the steady state, incompressible Newtonian Poiseuille flow in horizontal tubes and channels with Navier slip at the wall under the assumption of negligible gravity. In the case of a circular tube, the governing equations are non-dimensionalized by scaling the coordinates r^* and z^* by the tube radius R^*, the velocity vector $\mathbf{u}^*$ by the mean axial velocity U^*, and the pressure p^* and the stress tensor components by $\mu^* U^*/R^*$. Similar scalings are used in the planar case. It should be made clear that in order to be consistent with the flow development literature, the development lengths and the two

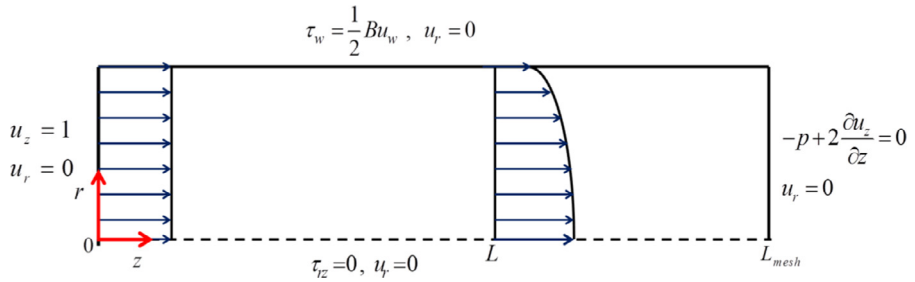

Fig. 1. Development of axisymmetric Poiseuille flow with wall slip: geometry and boundary conditions.

relevant dimensionless numbers, i.e. the Reynolds and the slip numbers, are defined using as length scale the diameter D^* instead of the radius R^*. The dimensionless continuity and momentum equations then read

$$\nabla \cdot \mathbf{u} = 0 \tag{5}$$

and

$$\frac{1}{2} Re\ \mathbf{u} \cdot \nabla \mathbf{u} = -\nabla p + \nabla^2 \mathbf{u}, \tag{6}$$

(the factor 1/2 is obviously due to the use of different scales used for the lengths and the Reynolds number). The geometry and the boundary conditions for the axisymmetric flow are depicted in Fig. 1. The origin is at the inlet and the length L_{mesh} of the flow domain is assumed to be sufficiently high so that the flow at the exit plane is fully developed. Hence $L_{mesh} >> 2L$ (recall that z^* is scaled by R^* whereas L^* is scaled by D^*). As for the boundary conditions at the inlet plane ($z = 0$), the axial velocity component is uniform and the radial one vanishes, i.e. $u_z = 1$ and $u_r = 0$. At the axis of symmetry ($r = 0$), the usual symmetry conditions apply, i.e. $\partial u_z/\partial r = 0$ and $u_r = 0$. At the outlet plane ($z = L_{mesh}$), the normal stress is assumed to vanish, i.e. $-p + 2\partial u_z/\partial z = 0$ and $u_r = 0$. Finally at the wall ($r = 1$), the radial velocity component is set to zero, $u_r = 0$ (no penetration), and the axial velocity component satisfies the Navier slip equation, the dimensionless form of which is

$$\tau_w = \frac{1}{2} B u_w \tag{7}$$

where

$$B \equiv \frac{\beta^* D^*}{\mu^*} \tag{8}$$

is the dimensionless slip number, which is the reciprocal of the dimensionless number used by Ferrás et al. [1].

The fully-developed velocity profile in a circular tube is

$$u_z(r) = \frac{8}{B+8} + \frac{2B}{B+8}\left(1 - r^2\right) \tag{9}$$

and thus the centerline and slip velocities are given by

$$u_c = \frac{2(B+4)}{B+8} \tag{10}$$

and

$$u_w = \frac{8}{B+8} \tag{11}$$

respectively. It is interesting to note that $u_c + u_w = 2$ independently of the value of the slip number B. This is not true, however, for the channel, in which case the fully-developed velocity profile is

$$u_x(y) = \frac{6}{B+6} + \frac{3B}{2(B+6)}\left(1 - y^2\right) \tag{12}$$

and thus

$$u_c = \frac{3(B+4)}{2(B+6)} \tag{13}$$

and

$$u_w = \frac{6}{B+6} \tag{14}$$

Table 1
Characteristics of short meshes ($L_{mesh} = 20$).

	Number of elements	Number of unknowns	Size of smallest element
Mesh 1	4844	44,605	0.019
Mesh 2	18,102	165,287	0.005
Mesh 3	42,581	387,823	0.002

Table 2
Convergence of development lengths in the case of planar flow. The wall development length L_w is defined only for $B < 792$. The results for $Re = 100$ are shown only for comparison purposes (a longer mesh is needed in this case).

B	Re	Mesh 1		Mesh 2		Mesh 3	
		L	L_w	L	L_w	L	L_w
∞	**0**	0.62857		0.62855		0.62854	
	0.001	0.62857		0.62856		0.62855	
	5	0.69250		0.69252		0.69252	
	100	4.65274		4.65279		4.65279	
10,000	**0**	0.62866		0.62864		0.62863	
	0.001	0.62867		0.62865		0.62864	
	5	0.69262		0.69264		0.69265	
	100	4.65319		4.65324		4.65324	
1000	**0**	0.62949		0.62947		0.62947	
	0.001	0.62950		0.62948		0.62948	
	5	0.69375		0.69377		0.69378	
	100	4.65728		4.65733		4.65733	
100	**0**	0.63784	0.65491	0.63782	0.65498	0.63783	0.65497
	0.001	0.63785	0.65491	0.63783	0.65498	0.63783	0.65497
	5	0.70537	0.70688	0.70538	0.70686	0.70537	0.70686
	100	4.70521	5.44265	4.70526	5.44244	4.70526	5.44375
10	**0**	0.68185	0.73632	0.68185	0.73635	0.68185	0.73635
	0.001	0.68186	0.73633	0.68186	0.73636	0.68186	0.73636
	5	0.78019	0.83138	0.78021	0.83139	0.78021	0.83138
	100	5.22759	5.81550	5.22762	5.81547	5.22762	5.81547
1	**0**	0.55650	0.58412	0.55649	0.58412	0.55649	0.58412
	0.001	0.55652	0.58414	0.55651	0.58414	0.55651	0.58414
	5	0.67971	0.70897	0.67971	0.70897	0.67971	0.70896
	100	4.69073	4.89348	4.69073	4.89347	4.69073	4.89347

3. Numerical results and discussion

The system of the governing equations and the boundary conditions presented in Section 2 was solved numerically using the finite element method (u-v-p formulation) with standard biquadratic basis functions for the two velocity components and bilinear ones for the pressure field. The Galerkin forms of the continuity and the momentum equations were used. The resulting nonlinear system of the discretized equations was solved with a Newton-Raphson iterative scheme with a convergence tolerance equal to 10^{-4}. Results have been obtained for Reynolds numbers in the range [0, 400] and slip numbers as low as 0.01. It should be noted that the wall development length has a meaning only in the presence of slip. A critical value of the slip number beyond which L_w is not definable can be found by demanding that 1% of the fully-developed slip velocity given by Eqs. (11) or (14) is equal to the convergence tolerance of 10^{-4} used in the numerical calculations. We thus find that the maximum values of B for the definition of L_w are 792 and 594 for the axisymmetric and planar flows, respectively. As discussed below, lower bounds for the slip number can be determined numerically as the values corresponding to full slip, i.e. to zero development length.

The convergence of the numerical results has been studied using both uniform and non-uniform meshes of different refinement. In the non-uniform meshes, the element size was reduced geometrically towards the inlet plane and towards the wall. Hence, the smallest element was at the inlet adjacent to the wall. Care was also taken so that meshes were sufficiently refined in the development region in order to get accurate estimates of the development lengths. The characteristics of three graded meshes of length $L_{mesh} = 20$, referred as Meshes 1, 2, and 3, are tabulated in Table 1.

In Table 2, we tabulate the values of the development lengths for the planar flow obtained with Meshes 1–3 for the same values of the Reynolds and slip numbers employed by Ferrás et al. [1]. As already mentioned, the wall development length is defined only below a critical value of the slip number ($B < 792$). Moreover, the results for $Re = 100$ are provided only for the sake of comparison, since a longer mesh is needed in this case. It should be noted that the convergence of the results has also been validated using uniform meshes of different refinements; the results obtained with Mesh 3 and a uniform mesh of element size 0.02 coincided up to four decimal digits. It can be seen that as slip becomes stronger (i.e. as

Table 3
Convergence of development lengths in the case of axisymmetric flow. The wall development length L_w is defined only for $B < 792$. The results for $Re = 100$ are shown only for comparison purposes (a longer mesh is needed in this case).

B	Re	Mesh 1		Mesh 2		Mesh 3	
		L	L_w	L	L_w	L	L_w
∞	**0**	0.60230		0.60230		0.60229	
	0.001	0.60232		0.60231		0.60231	
	5	0.70553		0.70552		0.70551	
	100	5.70688		5.70663		5.70663	
10,000	**0**	0.60239		0.60239		0.60239	
	0.001	0.60241		0.60241		0.60240	
	5	0.70564		0.70563		0.70562	
	100	5.70659		5.70635		5.70635	
1000	**0**	0.60321		0.60322		0.60321	
	0.001	0.60323		0.60323		0.60323	
	5	0.70659		0.70657		0.70657	
	100	5.70410		5.70386		5.70386	
100	**0**	0.61145	0.55374	0.61148	0.55372	0.61148	0.55370
	0.001	0.61147	0.55375	0.61150	0.55373	0.61150	0.55372
	5	0.71640	0.64543	0.71634	0.64545	0.71635	0.64546
	100	5.68735	5.32154	5.68712	5.32128	5.68712	5.32127
10	**0**	0.65154	0.59989	0.65156	0.59989	0.65156	0.59989
	0.001	0.65156	0.59991	0.65158	0.59991	0.65158	0.59991
	5	0.76887	0.69911	0.76885	0.69914	0.76886	0.69914
	100	5.64359	4.94664	5.64343	4.94662	5.64343	4.94662
1	**0**	0.54133	0.42567	0.54131	0.42566	0.54132	0.42567
	0.001	0.54135	0.42569	0.54133	0.42568	0.54133	0.42568
	5	0.64610	0.50095	0.64610	0.50095	0.64610	0.50095
	100	4.35576	3.06027	4.35565	3.06027	4.35565	3.06027

Table 4
Convergence of development lengths with meshes of different length when $Re = 100$ in the case of planar flow. The values obtained with $L_{mesh} = 120$ are converged up to five significant digits.

B	$L_{mesh} = 20$		$L_{mesh} = 60$		$L_{mesh} = 120$	
	L	L_w	L	L_w	L	L_w
∞	4.65279		4.67639		4.67644	
10,000	4.65324		4.67687		4.67687	
1000	4.65733		4.68125		4.68125	
100	4.70526	5.44375	4.73237	5.49004	4.73237	5.49205
10	5.22762	5.81547	5.30573	5.93326	5.30573	5.93326
1	4.69073	4.89347	4.91568	5.14437	4.91571	5.14441

B is reduced) convergence is achieved even with coarse meshes due to the fact that velocity gradients decrease and thus fewer elements are needed in resolving the flow. The convergence of the results with mesh refinement is much faster than that obtained by Ferrás et al. [1], who employed the finite volume method and resorted to Richardson extrapolation to get extrapolated converged values for the development length. Table 3 shows similar results for the axisymmetric flow.

In Table 4, we present the development lengths for $Re = 100$, calculated using Mesh 3 and its longer counterparts with $L_{mesh} = 60$ and 120. It is clear that the results with $L_{mesh} = 120$ are converged up to 5 significant digits and therefore no extrapolation is required for extracting converged values of the development lengths. Again convergence is accelerated as B is reduced. Table 5 shows similar results for the axisymmetric flow. The results of this section have been obtained using Mesh 3 for $Re \leq 40$ and its version with $L_{mesh} = 120$ for $40 \leq Re \leq 400$.

In Table 6, we compare our converged (i.e. mesh-independent) values of the development length L with the extrapolated values of Ferrás et al. [1]. The converged results for the axisymmetric flow are also shown. The calculated value of $L = 0.6286$ for the planar case with no-slip and $Re = 0$ agrees well with the value of 0.6284 provided by Ferrás et al. [1] for $Re = 0.001$ and is close to the value $L = 0.625$ proposed by Atkinson et al. [9]. Its axisymmetric counterpart $L = 0.6023$ is in agreement with the value $L = 0.6$ reported in the early works of Friedman et al. [8] and Goldberg and Folk [21], while Atkinson et al. [9] reported the value $L = 0.59$. It should be noted that in early works of flow development emphasis was put on high-Reynolds-number solutions rather than on those for the creeping case.

The discrepancies from the extrapolated values of Ferrás et al. [1] observed in Table 6 when the Reynolds number is non-zero and slip is applied are due to the limitations of the finite volume method and the errors associated with the use of Richardson's extrapolation with non-uniform meshes. It should also be pointed out that implementing a slip law relating

Table 5
Convergence of development lengths with meshes of different length when $Re = 100$ in the case of axisymmetric flow. The values obtained with $L_{mesh} = 120$ are converged up to five significant digits.

B	$L_{mesh} = 20$		$L_{mesh} = 60$		$L_{mesh} = 120$	
	L	L_w	L	L_w	L	L_w
∞	5.70663		5.80733		5.80733	
10,000	5.70635		5.80703		5.80703	
1000	5.70386		5.80438		5.80438	
100	5.68712	5.32127	5.78670	5.39989	5.78669	5.39988
10	5.64343	4.94662	5.74559	5.01205	5.74559	5.01205
1	4.35565	3.06027	4.41362	3.08613	4.41362	3.08613

Table 6
Converged values of the development length L for both the planar and the axisymmetric flows. In the former case, the values reported by Ferrás et al. (2012) are also provided.

B	Re	Planar flow		Axisymmetric flow
		Present work	Ferrás et al. [1]	Present work
No slip	**0.001**	0.6286		0.6023
	5	0.6925		0.7055
	100	4.6764		5.8073
10,000	**0.001**	0.6286	0.6284	0.6024
	5	0.6926	0.6934	0.7056
	100	4.6769	4.6912	5.8070
1000	**0.001**	0.6295	0.6293	0.6032
	5	0.6938	0.6945	0.7066
	100	4.6813	4.6955	5.8044
100	**0.001**	0.6378	0.6377	0.6115
	5	0.7054	0.7065	0.7164
	100	4.7324	4.7474	5.7867
10	**0.001**	0.6819	0.6816	0.6516
	5	0.7802	0.7811	0.7689
	100	5.3057	5.3179	5.7456
1	**0.001**	0.5565	0.5560	0.5413
	5	0.6797	0.6799	0.6461
	100	4.9157	4.9180	4.4136

explicitly the wall shear stress to the slip velocity is straightforward in a finite-element formulation but requires special treatment with the finite-volume method. Ferrás et al. [1] report a method of an accuracy error below 1%. Moreover, they did not consider for the limiting cases of $Re = 0$ (creeping flow) and $B \to \infty$ (no-slip), obtaining results for $Re = 0.001$ and $B = 10{,}000$, respectively, and extrapolating to the corresponding limit.

The combined effects of slip and inertia on the flow development for both the axisymmetric and planar flows are illustrated in Fig. 2, where L (solid lines) and L_w (dotted lines) are plotted versus the slip number B for various values of the Reynolds number: $Re = 0$, 5, 10, and 20. Since it is not defined when slip is very weak, L_w is not calculated at high values of the slip number. The fact that the development length increases with the Reynolds number is expected and well-known [1,11]. Moreover, as slip is increased, that is as B is reduced from infinity (no slip), the development length increases slightly initially and then more rapidly passing through a maximum when slip is moderate (B is between 1 and 10) after which it is reduced vanishing at a finite value of B. The existence of a maximum for L in the case of the planar flow was reported by Ferrás et al. [1], who also noted that the maximum slightly moves to the left as Re is increased (Fig. 2b). (With their definition of the slip number the maximum actually moves to the left.) Comparing Fig. 2a and b we observe that in the axisymmetric case the maximum moves slightly to the right as the Reynolds number is increased. An interesting observation is that the wall development length is smaller than L only in the axisymmetric case, i.e., in the planar case with finite wall slip the flow near the wall develops more slowly than at the plane of symmetry. As discussed below, for a small range of slip numbers above the critical value at which both L and L_w vanish, L_w is actually bigger than L. In the planar case $L_w > L$ for slip numbers up to about 100, which implies that in the presence of moderate slip the flow develops slower at the wall than at the midplane. Moreover, the maxima in L_w are sharper than those in L while in the axisymmetric case they are not as sharp. In fact, the wall development length for $Re = 20$ is monotonic in the latter case.

Another difference is revealed when calculating the critical slip number for full slip, which is the slip number at which both development lengths are zero. In Fig. 2a, we observe that in the axisymmetric flow both L and L_w vanish roughly at the same critical slip number. More specifically, L and L_w vanish at $B_c = 0.0816$ and $B_{wc} = 0.0810$, respectively. Obviously, in the region of such small slip numbers, L_w becomes higher than L. Hence, for the latter value of the slip number, the flow is essentially uniform everywhere (full slip). In the planar case, however, the critical slip number values at which L and L_w vanish defer considerably: $B_c = 0.1236$ and $B_{wc} = 0.0606$. The evolution of the centerline and slip velocities for the above

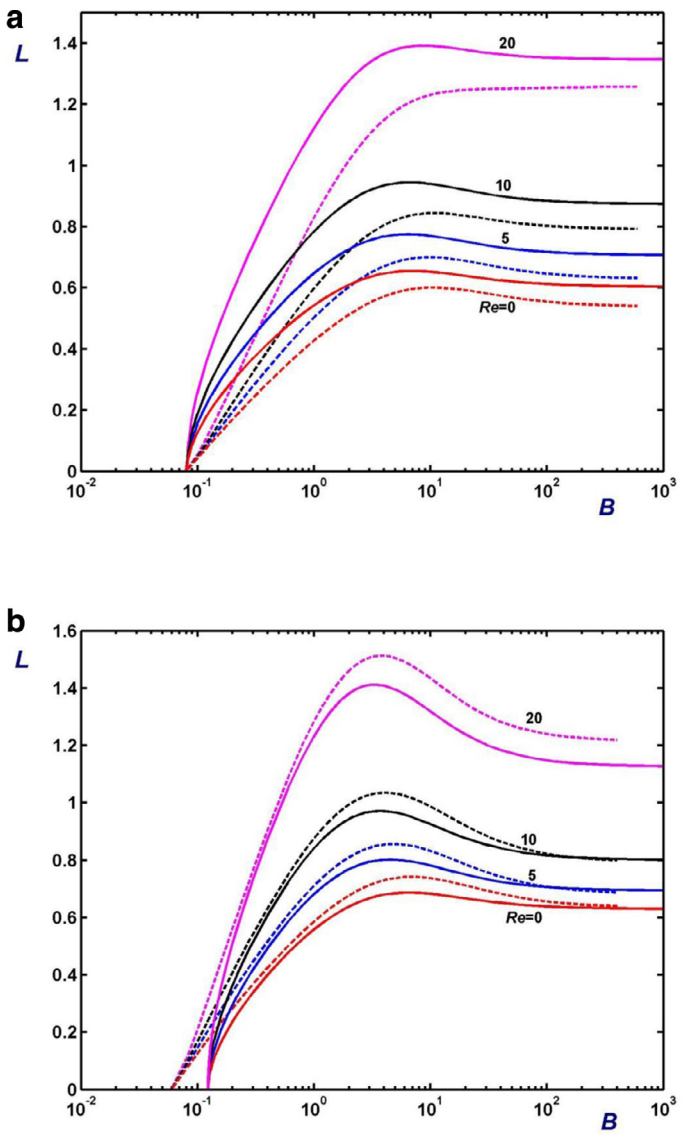

Fig. 2. Development length as a function of the slip number for various Reynolds numbers: (a) axisymmetric flow; (b) planar flow. The dashed lines correspond to the wall development length, L_w, which is defined only below a critical slip number (792 and 594 for the axisymmetric and planar flows, respectively). In the planar case, L_w is greater than L, which implies that in the presence of slip the flow develops more slowly near the wall.

critical values of the slip number is illustrated in Fig. 3. In the axisymmetric flow both u_w and u_c lie in the interval [0.99 1.01] for $B = B_{wc} = 0.0810$ and thus both development lengths are zero. In the planar case this is true for $B = B_{wc} = 0.0606$. For $B = B_c = 0.1236$, L is zero but L_w is about 0.738. In conclusion, the critical values of the slip number for full slip are 0.0810 and 0.0606 for the axisymmetric and planar geometries, respectively.

The effect of slip on the axisymmetric flow development is also illustrated in Fig. 4, where the centerline and slip velocities for $Re = 0$ and 100 are plotted for different values of the slip number, ranging from 0.2 (strong slip) to 200 (very weak slip). We observe again that in all cases the flow development region grows with the Reynolds number and the development length passes through a maximum (around $B \approx 2$) as the slip number is increased. The stars denote the points at which u_c and u_w are developed, i.e. the points corresponding to L and L_w (recall that these are scaled by D^* and not by R^*). Fig. 4 clearly shows that the slip velocity attains its fully-developed value earlier than its centerline counterpart for all values of the slip number. This is not the case with the results of Fig. 5 for the planar flow, where the fact that the flow development is slower at the wall than at the midplane ($L_w > L$) can again be observed.

Fig. 6 shows plots of the development length for $Re = 0$, 5, 10 and 100 versus $1/B$, which corresponds to the slip number employed by Ferrás et al. [1], together with their extrapolated results. As already noted, the converged results of the present work do not agree closely with the values provided by Ferrás et al. [1]. The discrepancies become more significant as the

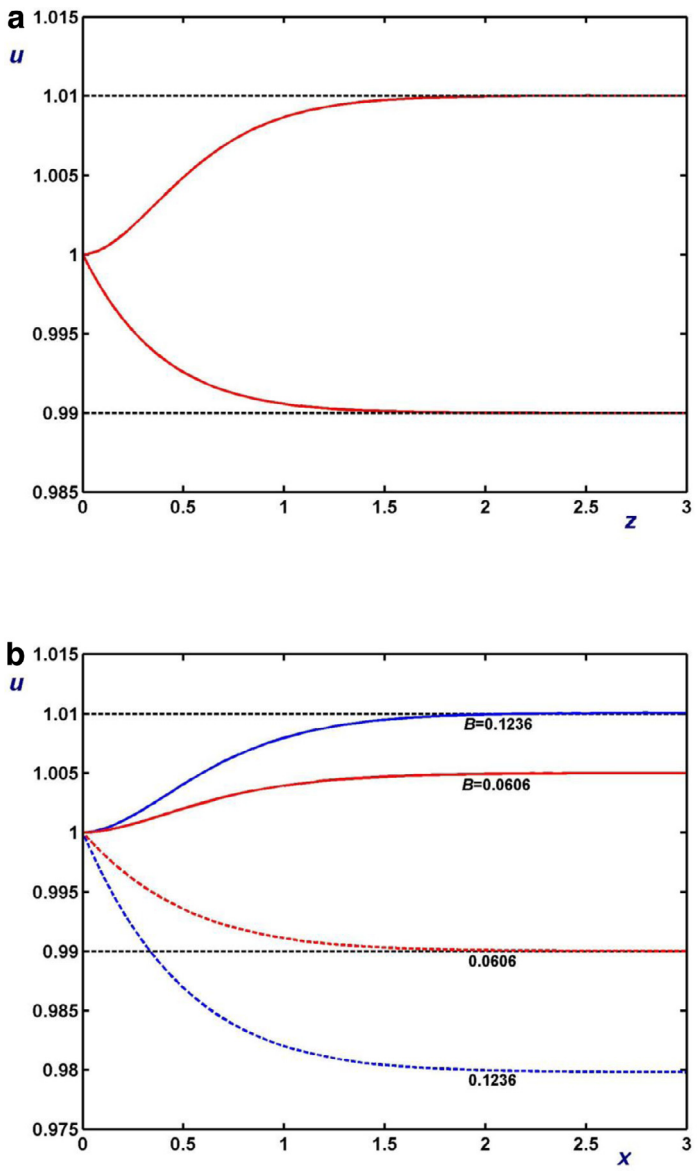

Fig. 3. Evolution of the centerline (solid) and slip (dotted) velocities in creeping flow ($Re = 0$) for the critical slip numbers corresponding to zero development lengths: (a) axisymmetric flow with $B = B_{wc} = 0.0810$ (L and L_w vanish at about the same critical slip number); (b) planar flow with $B = B_{wc} = 0.0606$ and $B = B_c = 0.1236$ (L_w vanishes at a lower slip number than L).

Reynolds number is increased. The wall development length is also shown for comparison purposes. Note again the crossing of the curves of L and L_w at high values of B (weak slip).

In Fig. 7, the development lengths for the planar flow are plotted versus the Reynolds number for various values of the slip number, i.e. for $B = 1$, 10, 100, and 1000. As already mentioned, at low Reynolds numbers L initially increases and then decreases with B. At high Reynolds numbers the curves cross each other indicating the competition of slip and inertia. The agreement with the values of Ferrás et al. [1] for L is again good but not very close. The wall development lengths for $B = 1$, 10 and 100, which are always bigger than their centerline counterparts, are also plotted. As already noted, the opposite is true for the axisymmetric flow (Fig. 8).

In all cases (see, e.g., Figs. 7 and 8), both L and L_w increase monotonically with the Reynolds number, exhibiting a plateau at low (less than 1) and a linear region at high Reynolds numbers (greater than 10). This behavior may be roughly described by Eq. (3), which however is not adequate in the intermediate regime of Reynolds numbers. Other models involving more parameters have been proposed for this reason, such as the one proposed by Durst et al. [11] for the no-slip case:

$$L = \left[(C_0)^n + (C_1 Re)^n\right]^{1/n} \tag{15}$$

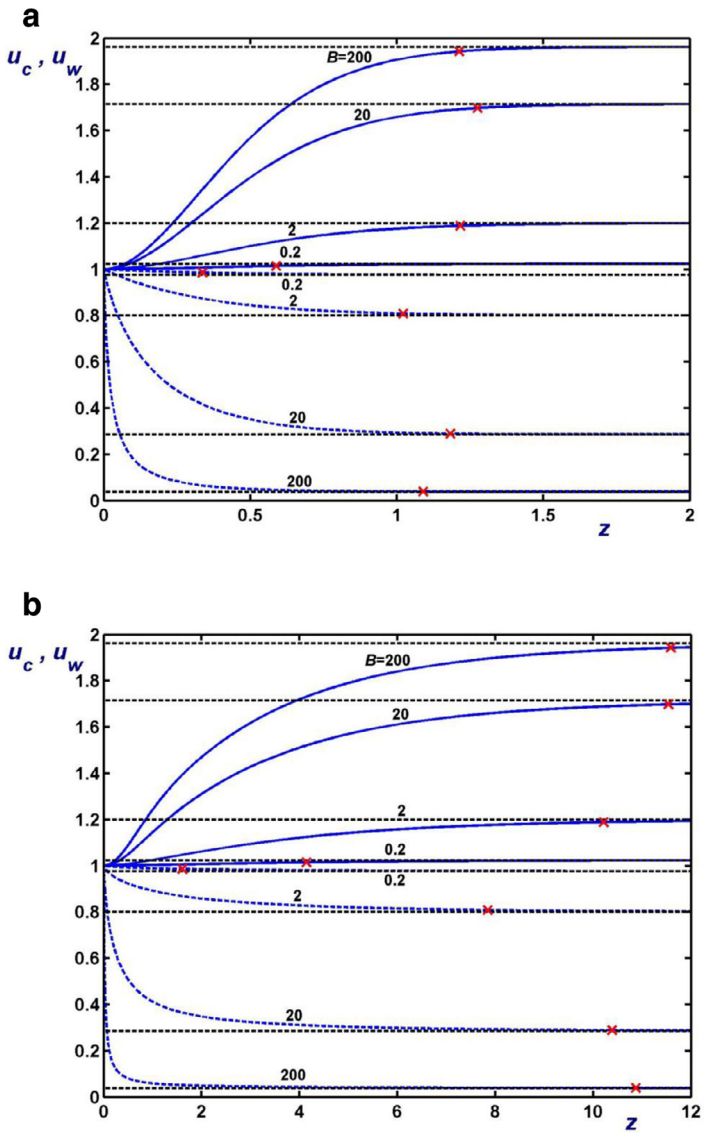

Fig. 4. Evolution of the centerline (solid) and slip (dashed) velocities in axisymmetric Newtonian flow for various slip numbers ranging from 0.2 (strong slip) to 200 (very weak slip): (a) $Re = 0$; (b) $Re = 100$. The horizontal dashed lines denote the fully-developed values given by Eqs. (10) and (11). The stars denote the points where u_c and u_w are developed, i.e. the points corresponding to L and L_w respectively. The slip velocity attains its fully-developed value earlier than the centerline velocity for all values of B.

An extension of the above model incorporating wall slip effects has also been proposed by Ferrás et al. [1] for the planar flow. Given that the optimal parameters of such a correlation depend on the Reynolds number range of interest and on the input data and their corresponding rather subjective weights, proposing an entrance length correlation is out of the scope of the present work.

The development of the axial velocity in a circular tube has been studied for various values of the Reynolds number ranging from 0 to 100. The results for the no-slip case agree well with previous results in the literature [8,9,21]. In Fig. 9, velocity profiles obtained with $Re = 100$ are plotted at different distances from the entrance for various slip numbers corresponding to no ($B = \infty$), weak ($B = 100$) and moderate ($B = 10$) slip (the fully-developed slip velocities are 0, 0.0741 and 0.4444, respectively). A well-known feature of the flow development is the appearance of an overshoot (kink) in the velocity profiles close to the tube entrance and near the wall and of a local minimum at the axis, which results in the concavity of the velocity profiles far from the wall. Shah and London [6] confirmed this phenomenon both experimentally and analytically. The velocity overshoot becomes less pronounced and eventually disappears as the flow develops downstream and the velocity profile tends to become parabolic. The kink is sharper and concavity is much more pronounced at higher Reynolds numbers [8,22]. As noted by Darbandi and Schneider [23], the velocity overshoot is due to the abrupt fluid deceleration

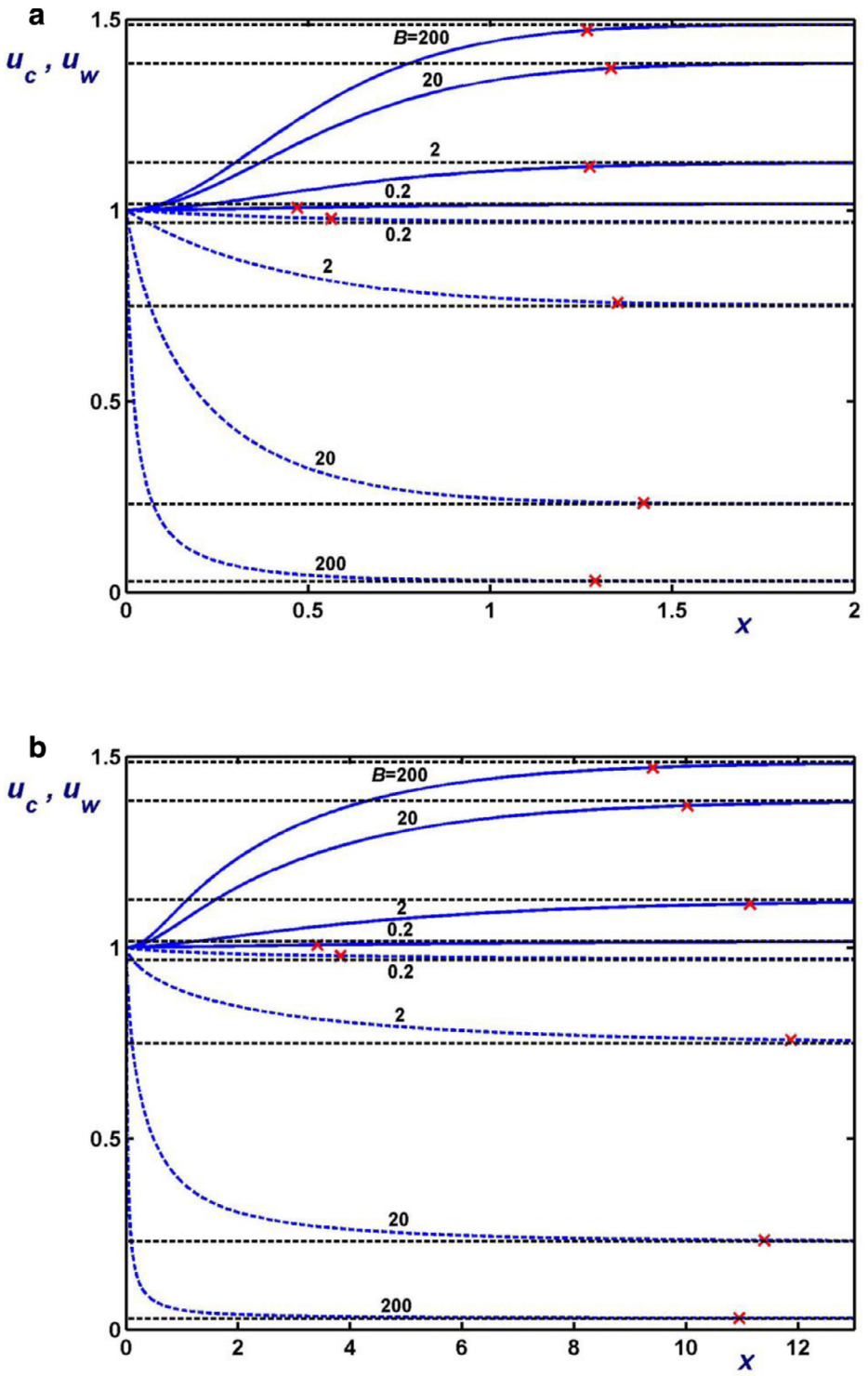

Fig. 5. Evolution of the centerline (solid) and slip (dashed) velocities in planar Newtonian flow for various slip numbers ranging from 0.2 (strong slip) to 200 (very weak slip): (a) $Re = 0$; (b) $Re = 100$. The horizontal dashed lines denote the fully-developed values given by Eqs. (13) and (14). The stars denote the points where u_c and u_w are developed, i.e. the points corresponding to L and L_w respectively. The slip velocity attains its fully-developed value later than the centerline velocity for all values of B.

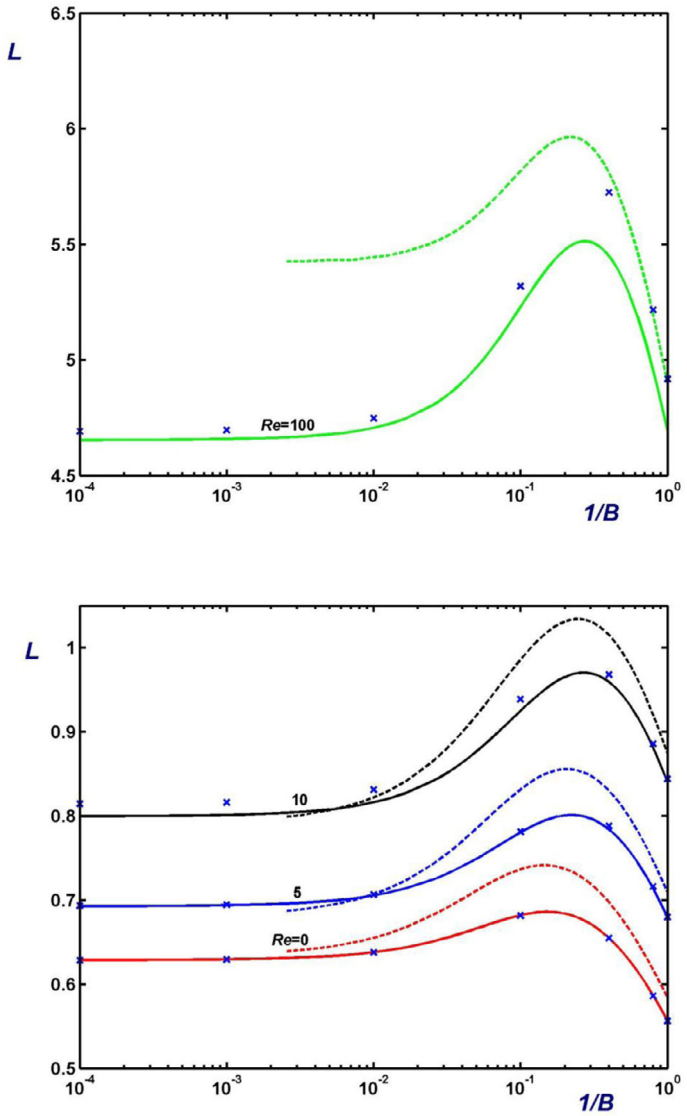

Fig. 6. Development lengths for the planar flow as a function of $1/B$ for various Reynolds numbers compared with the extrapolated values of Ferrás et al. [1] (symbols). The dashed lines correspond to the wall development length, L_w (which is defined only above a critical value of $1/B$).

near the wall which is faster than diffusion-induced momentum transport to the center plane. In the presence of slip, the deceleration of the fluid near the wall is not as abrupt and thus the overshoot is not as sharp, as already pointed out by Ferrás et al. [1] for the case of the planar flow.

The development of the velocity in a channel is quite similar, as it can be observed in Fig. 10 where results for $Re = 100$ and various slip numbers are shown. However, there is a notable difference due to the fact that the wall development length, L_w, is greater than L in the presence of slip. While in the circular tube case the velocity tends to reach the fully-developed profile faster near the wall than around the symmetry axis, the opposite phenomenon is observed in the channel.

In flow development in a circular tube with no-slip, the axial pressure has been reported to exhibit a maximum at a small distance from the entrance (see [10] and references therein). This effect is attributed to the higher wall shear stress and to the pressure gradients required for the rapid acceleration of the fluid in the near the wall regions. It should also be noted that the wall pressure at the entrance tends to become infinite due to the singularity introduced by the sudden change in the wall boundary condition. Therefore the wall pressure decays monotonically and merges downstream with the decreasing part of the axial pressure. The pressure at intermediate radial distances lies between the axial and wall curves. In the presence of slip, these phenomena are milder and hence the axial pressure maxima are less pronounced. This is illustrated in Fig. 11, where the axial and wall pressures for the creeping flow in a circular tube of length $L_{mesh} = 20$ are plotted for various slip numbers. As slip becomes stronger, i.e., as the slip number B is reduced, the required pressure

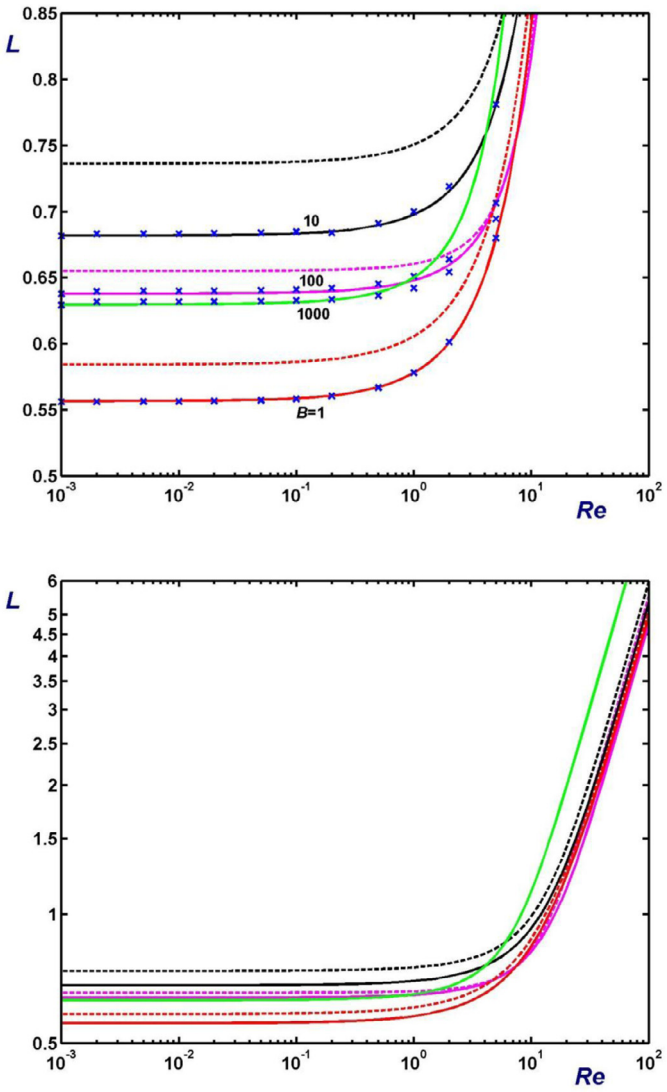

Fig. 7. Development length (solid) and wall development length (dotted) in the planar flow as a function of the Reynolds number for various slip numbers. The dashed lines correspond to the wall development length, L_w, which is always bigger than L. The symbols in the upper plot correspond to the extrapolated values of Ferrás et al. [1].

to drive the flow is reduced. It is interesting to note that the position of the pressure maximum is independent of the slip number; for $Re = 0$, $z_{\max} = 0.3128$. Our numerical calculations showed that the location of the axial pressure maximum moves towards the entrance and remains insensitive to slip as the Reynolds number is increased. The sharpness of the pressure peak, however, decreases with the Reynolds number, in agreement with previous works [10].

Another quantity of interest is the (dimensionless) excess pressure, p_e, which is usually defined as the difference between the actual pressure and the pressure corresponding to the fully developed flow [21,13]. With the symbols employed in the present work, one gets

$$p_e(r,z) = p(r,z) - \frac{8B}{B+8}(L_{mesh} - z) \tag{16}$$

for the circular tube and

$$p_e(x,y) = p(x,y) - \frac{3B}{B+6}(L_{mesh} - x) \tag{17}$$

for the channel. The axial ($r = 0$) and wall ($r = 1$) excess pressures in the case of creeping ($Re = 0$) flow development in a circular tube are plotted in Fig. 12 for various slip numbers corresponding to no-, moderate and strong slip ($B = \infty$, 100 and 1). The curve for $B = \infty$ agrees well with the results of Goldberg and Folk [21]. As expected, the excess pressure is reduced

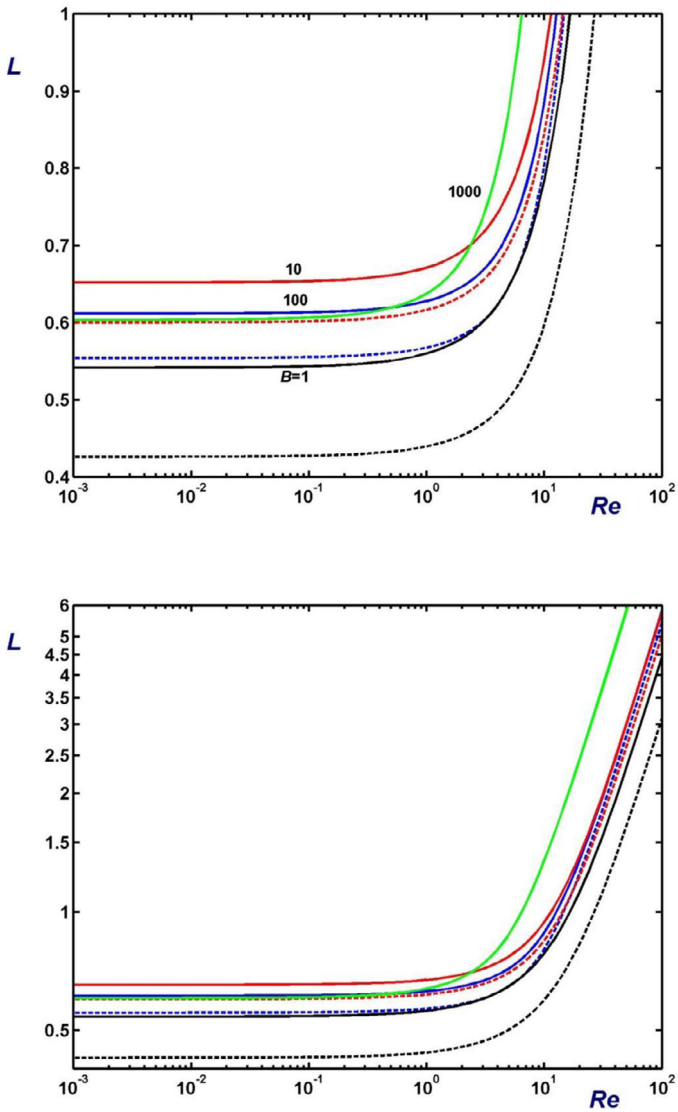

Fig. 8. Development length (solid) and wall development length (dotted) in the axisymmetric flow as a function of the Reynolds number for various slip numbers. The dashed lines correspond to the wall development length, L_w, which is smaller than L (in contrast to the planar flow).

in magnitude as slip becomes stronger. While the axial excess pressure decays faster initially, its decay may become slower downstream as slip becomes stronger, depending on the value of the slip number.

4. Conclusions

We have studied numerically the flow development of a Newtonian fluid in both channels and tubes, assuming that slip occurs following Navier's slip law. Two definitions of the development length have been considered, i.e. the standard centreline development length L and the wall development length L_w, which is relevant in the presence of non-weak slip. Results have been obtained for Reynolds numbers in the range $0 \leq Re \leq 400$ and for slip numbers in the range $0 \leq B < \infty$. The calculated values of L for the planar case are in good agreement with the results of Ferrás et al. [1]. Both L and L_w were found to be non-monotonic functions of the slip number passing through a maximum as the latter is increased. The most interesting finding of the present work is that the flow development in the channel is slower near the wall than at the midplane, i.e., $L_w > L$ in the presence of finite slip. Moreover, slip is found to suppress the velocity overshoot and the axial pressure maximum near the entrance. The extension of the present work to generalized Newtonian flows is the subject of our current investigations.

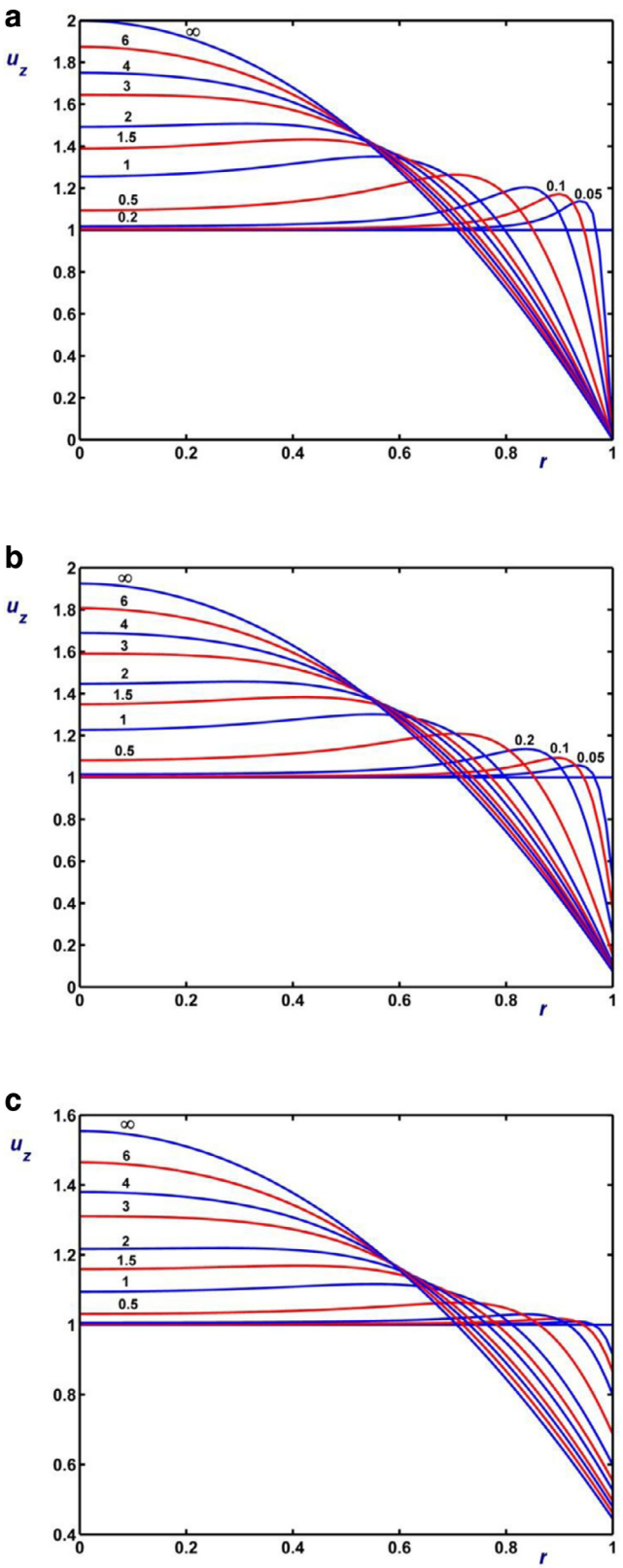

Fig. 9. Development of the velocity in a circular tube for $Re = 100$: (a) no-slip ($L = 5.807$ and $u_c^\infty = 2$); (b) $B = 100$ ($L = 5.787$, $L_w = 5.400$, $u_c^\infty = 1.9259$ and $u_w^\infty = 0.0741$); and (c) $B = 10$ ($L = 5.746$, $L_w = 5.012$, $u_c^\infty = 1.5556$ and $u_w^\infty = 0.4444$). In the presence of slip the velocity overshoot is suppressed and the velocity develops faster near the wall than at the axis of symmetry.

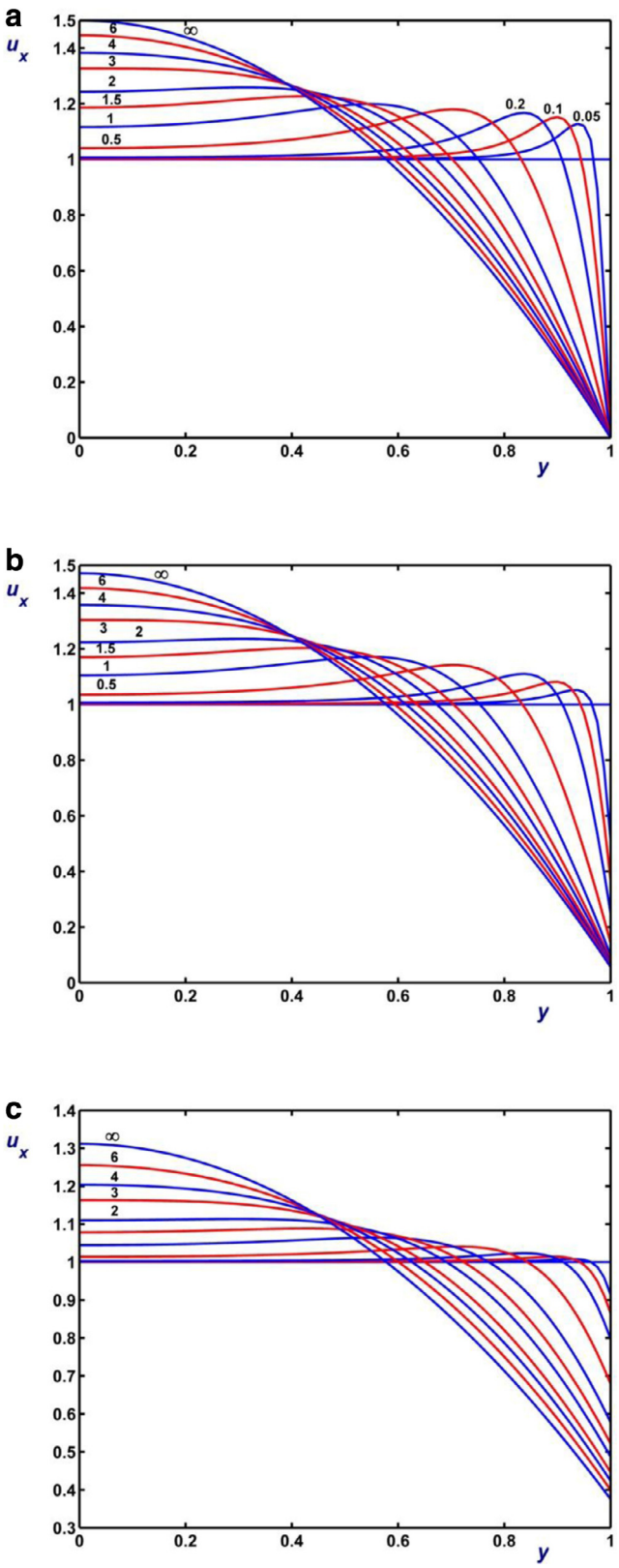

Fig. 10. Development of the velocity in a channel for $Re = 100$: (a) no-slip ($L = 4.676$ and $u_c^\infty = 1.5$); (b) $B = 100$ ($L = 4.732$, $L_w = 5.492$, $u_c^\infty = 1.4717$ and $u_w^\infty = 0.0566$); and (c) $B = 10$ ($L = 5.306$, $L_w = 5.933$, $u_c^\infty = 1.3125$ and $u_w^\infty = 0.3750$). In the presence of slip the velocity overshoot is suppressed and the velocity develops faster at the symmetry plane than at the wall.

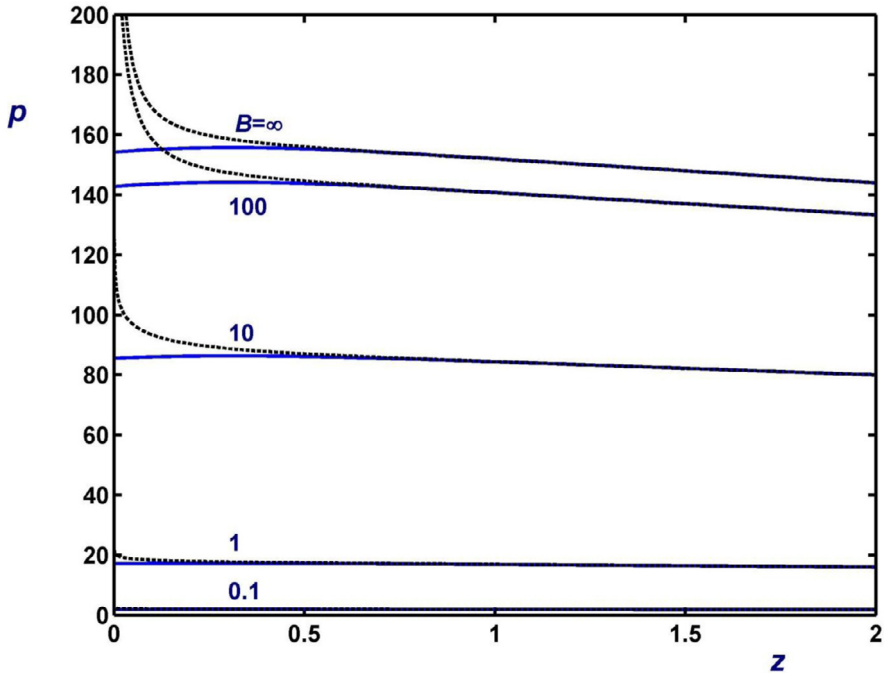

Fig. 11. Axial (solid) and wall (dashed) pressures for various slip numbers in the case of creeping ($Re = 0$) flow development in circular tube ($L_{\text{mesh}} = 20$). The wall pressure, which is infinite initially due to the singularity at the entrance corner, decays and merges with the axial pressure downstream. Slip suppresses the maximum of the axial pressure observed at a small distance from the entrance.

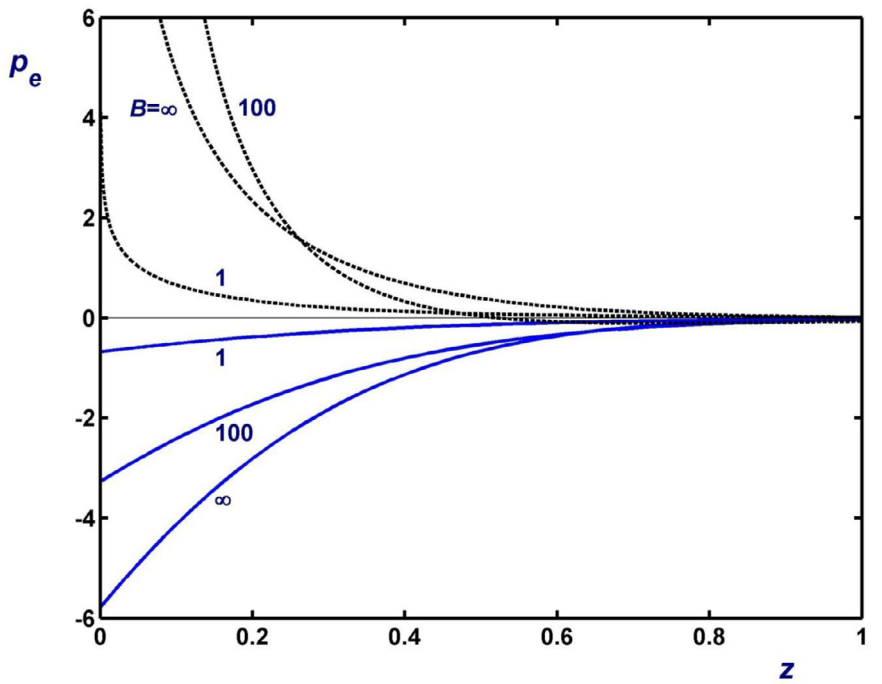

Fig. 12. Axial (solid) and wall (dashed) excess pressures for $B = \infty$ (no slip), 100 (moderate slip) and 1 (strong slip) in the case of creeping ($Re = 0$) flow development in circular tube ($L_{\text{mesh}} = 20$). One observes that the axial excess pressure decreases with wall slip.

References

[1] L.L. Ferrás, A.M. Afonso, J.M. Nóbrega, M.A. Alves, F.T. Pinho, Development length in planar channel flows of Newtonian fluids under the influence of wall slip, ASME J. Fluids Eng. 134 (2012) 104503.
[2] A. Sinclair, Steady and Oscillatory Flow in the Entrance Region of Microchannels PhD Thesis, The University of New South Wales, 2012.
[3] A.G. Darbyshire, T. Mullin, Transition to turbulence in constant-mass-flux pipe flow, J. Fluid Mech. 289 (1995) 83–114.
[4] C. Neto, D.R. Evans, E. Bonaccurso, H.J. Butt, V.S. Craig, Boundary slip in Newtonian liquids: a review of experimental studies, Rep. Progr. Phys. 68 (2005) 2859–2897.
[5] T. Ahmad, I. Hassan, Experimental analysis of microchannel entrance length characteristics using microparticle image velocimetry, ASME J. Fluids Eng. 132 (2010) 041102.
[6] R. Shah, A. London, Laminar Flow Forced Convection in Ducts: a Source Book for Compact Heat Exchanger Analytical Data, Academic Press, New York, 1978.
[7] D. Fargie, B. Martin, Developing laminar flow in a pipe of circular cross-section, Procs. Royal. Soc. London A. 321 (1971) 461–476.
[8] M. Friedmann, J. Gillis, N. Liron, Laminar flow in a pipe at low and moderate Reynolds numbers, Appl. Sci. Res. 19 (1968) 426–438.
[9] B. Atkinson, M.P. Brocklebank, C.C.H. Card, J.M. Smith, Low Reynolds number developing flows, AIChE J. 15 (1969) 548–553.
[10] N. Dombrowski, E.A. Foumeny, S. Ookawara, A. Riza, The influence of Reynolds number on the entry length and pressure drop for laminar pipe flow, Can. J. Chem. Eng. 71 (1993) 472–476.
[11] F. Durst, S. Ray, B. Unsal, O.A. Bayoumi, The development lengths of laminar pipe and channel flows, ASME J. Fluids Eng. 127 (2005) 1154–1160.
[12] D. Boger, Circular entry flows of inelastic and viscoelastic fluids, Adv. Transp. Process. 2 (1982) 43–104.
[13] R.I. Tanner, Engineering Rheology, second ed., Oxford University Press, Oxford, UK, 2000.
[14] R.J. Poole, B.S. Ridley, Development-length requirements for fully developed laminar pipe flow of inelastic non-Newtonian liquids, ASME J. Fluids Eng. 129 (2007) 1281–1287.
[15] R.J. Poole, R.P. Chhabra, Development length requirements for fully developed laminar pipe flow of yield stress fluids, ASME J. Fluids Eng. 132 (2010) 034501.
[16] L.L. Ferrás, C. Fernandes, O. Pozo, A.M. Afonso, M.A. Alves, J.M. Nóbrega, F.T. Pinho, Development length in channel flows of inelastic fluids described by the Sisko viscosity model, in: V Conferencia Nacional de Mecanica dos Fluidos, Termodinamica e Energia MEFTE, Porto, 11-12 September, 2014.
[17] K. Yapici, B. Karasozen, Y. Uludag, Numerical analysis of viscoelastic fluids in steady pressure-driven channel flow, ASME J. Fluids Eng. 134 (2012) 051206.
[18] C.L.M.H. Navier, Sur les lois de mouvement des fluides, Mem. Acad. R. Sci. Inst. Fr. 6 (1827) 289–440.
[19] M.M. Denn, Extrusion instabilities and wall slip, Ann. Rev. Fluid Mech. 33 (2001) 265–287.
[20] Z. Duan, Y.S. Muzychka, Slip flow in the hydrodynamic entrance region of circular and noncircular microchannels, ASME J. Fluids Eng. 132 (2010) 011201.
[21] I.S. Goldberg, R.T. Folk, Solutions for steady and nonsteady entrance flow in a semi-infinite circular tube at very low Reynolds numbers, SIAM J. Appl. Math. 48 (1988) 770–791.
[22] M.H. Wagner, Developing flow in circular conduits: Transition from plug flow to tube flow, J. Fluid Mech. 72 (1975) 257–268.
[23] M. Darbandi, G.E. Schneider, Numerical study of the flow behavior in the uniform velocity entry flow problem, Num. Heat Transfer, Part A 34 (1988) 479–494.